ELSEVIER

Journal of Biomechanics 33 (2000) 35–43

JOURNAL OF BIOMECHANICS

www.elsevier.com/locate/jbiomech

Biomechanics of cell rolling: shear flow, cell-surface adhesion, and cell deformability

Cheng Dong*, Xiao X. Lei

Bioengineering Program, The Pennsylvania State University, 229 Hollowell Building, University Park, PA 16802, USA

Abstract

The mechanics of leukocyte (white blood cell; WBC) deformation and adhesion to endothelial cells (EC) has been investigated using a novel in vitro side-view flow assay. HL-60 cell rolling adhesion to surface-immobilized P-selectin was used to model the WBC–EC adhesion process. Changes in flow shear stress, cell deformability, or substrate ligand strength resulted in significant changes in the characteristic adhesion binding time, cell–surface contact and cell rolling velocity. A 2-D model indicated that cell–substrate contact area under a high wall shear stress (20 dyn/cm^2) could be nearly twice of that under a low stress (0.5 dyn/cm^2) due to shear flow-induced cell deformation. An increase in contact area resulted in more energy dissipation to both adhesion bonds and viscous cytoplasm, whereas the fluid energy that inputs to a cell decreased due to a flattened cell shape. The model also predicted a plateau of WBC rolling velocity as flow shear stresses further increased. Both experimental and computational studies have described how WBC deformation influences the WBC–EC adhesion process in shear flow.

Keywords: Transient adhesion; Side-view flow assay; Modeling

1. Introduction

Selectins are responsible for "capturing" or "tethering" leukocytes (white blood cells; WBC) in post capillary venules (Springer, 1994). Selectin-mediated WBC rolling at physiologic flow rates was found to be a distinct prerequisite for integrin-mediated final WBC arrest to endothelium (EC) (Lawrence and Springer, 1991). Such a process involves a complex balance of forces arising from hydrodynamic shearing effects and the strength of the adhesive bond between the WBC and EC (Lauffenberger and Linderman, 1993). Hydrodynamics appears to play an important role in allowing cell rolling to occur by driving the cells forward while the specific adhesion force holds them at the marginal position of the vessel. The rheological properties of WBC alter the circumstances under which both WBC–EC adhesion bond forces and fluid shear forces act. Cell deformation contributes to a stronger WBC–EC adhesion by providing a larger contact area so that more adhesion receptor–ligand pairs can be formed. As a cell elongates, a decrease in cell height results in less vessel-lumen obstruction and less fluid driving force on the cell. This suggests the importance of cell deformability and its potential role in regulating WBC–EC interactions.

In the present study, HL-60 cell rolling adhesion to surface-immobilized P-selectin in shear flow has been investigated using a newly developed side-view flow chamber (Cao et al., 1997), which permits measurements of cell deformation and cell–substrate contact length as well as cell rolling velocity. The purified P-selectin was coated onto a clean microslide surface to simulate the vascular endothelium. HL-60 cells were chosen because they express levels of PSGL-1 (P-selectin ligand) comparable to that on most human leukocytes. A two-dimensional model was recently developed based on an assumption that the fluid energy input to a rolling cell would be essentially distributed into two parts: cytoplasmic viscous dissipation, and an energy needed to break adhesion bonds between the rolling cell and its substrate (Lei et al., 1999). Both extracellular and intracellular flow fields were solved using finite element methods with a deformable cell membrane represented by an elastic ring. The adhesion energy loss was calculated based on the receptor–ligand kinetic equations. It was found that the cell-substrate contact area under high wall shear stresses (20 dyn/cm^2) could be nearly twice of that under

* Corresponding author. Tel.: 814-865-1407; fax: 814-863-0490.
E-mail address: cxd23@psu.edu (C. Dong)

0021-9290/99/$ - see front matter
PII: S0021-9290(99)00174-8

low stresses (0.5 dyn/cm^2) as a result of shear flow-induced cell deformation. An increase in contact area results in more energy dissipation to both adhesion bonds and viscous cytoplasm whereas the fluid energy that inputs to the rolling cell might decrease due to the flattened cell shape, indicating how WBC deformation influences the WBC–EC adhesion process in shear flow.

2. Materials and methods

Human promyelocytic leukemic cell lines (HL-60) were maintained in tissue culture as detailed elsewhere (Lei et al., 1999).

The side-view flow chamber consisted of two precision rectangular glass tubes called microslides (Fig. 1a). The smaller microslide was inserted into a larger one to create a flow channel with a flat surface on which the selected P-selectin molecules were present. Two optical prisms, each with a 45° chromium-coated surface, were used along the flow channel to generate side-view light illumination. This design allowed the measurement of cell rolling velocity, cell shape change and cell-substrate contact length (Fig. 1b).

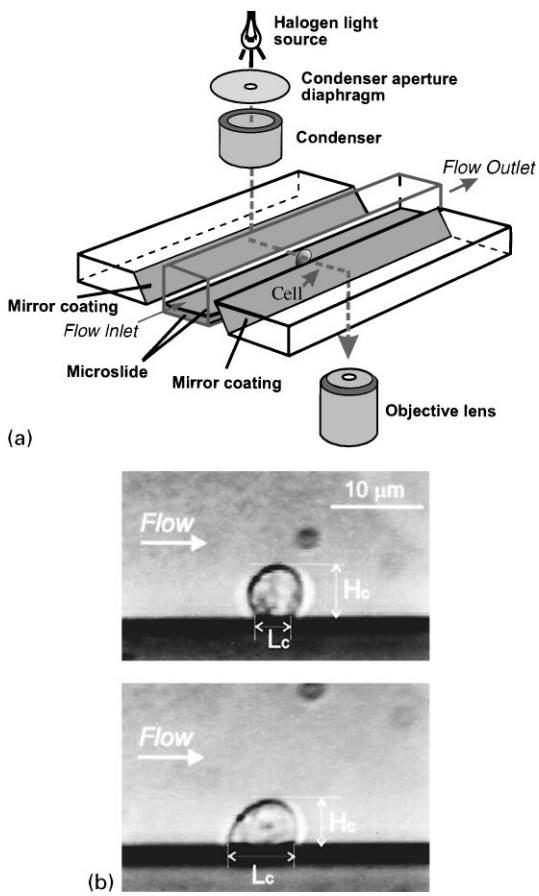

Fig. 1. (a) Schematic diagram of the side-view flow chamber setup. Light from the condenser is first reflected by one of the 45° prisms, through the cell-substrate interface, and then reflected by another 45° prism to reach the objective lens, (b) Side-view images of HL-60 cells rolling on P selectin-coated substrate. For the particular images shown, P-selectin density is 3.75×10^{10} sites/cm^2. The inlet wall shear stress is 2 (top) and 15 (bottom) dyn/cm^2, respectively.

P-selectin was purified from outdated blood platelets by immunoaffinity chromatography, which was generously provided by Dr. Michael Lawrence (Univ. of Virginia, Charlottesville, VA). P-selectin molecules were adsorbed to the microslide surface following the method developed by Cao et al. (1998). Site density of adsorbed P-selectin on the glass surface as a function of P-selectin solution concentration was determined by a radioimmunoassay using a functional blocking monoclonal antibody G1 (Lawrence et al., 1997).

To increase cell deformability, HL-60 cells were treated with 10 μM cytochalasin B (CB; Sigma, St. Louis, MO) before any flow assays. The cell suspension was then perfused through the flow channel over the P-selectin immobilized substrate using a syringe pump (Harvard Apparatus, MA). The rolling adhesion of HL-60 cells on P-selectin was observed through an inverted microscope (Nikon, Melville, NY). The effects of flow shear stress, cell deformability, and substrate P-selectin density on HL-60 cell deformation and rolling adhesion were analyzed.

3. Modeling and analyses

To understand the relative influence of shear flow, adhesion strength, and cell deformability on WBC rolling (Fig. 2a), a 2-D model was employed (Fig. 2b). An elastic ring enclosing an incompressible viscous fluid represented an actual 3-D cell. Adhesion bonds formed between WBC surface and its substrate were treated as elastic springs that were perpendicular to the substrate. For simplicity, WBC surface microvilli were neglected in the current model by assuming a smooth membrane surface. A prestressed elastic ring, with both adherent and non-adherent portions, simulated an actin-rich cell cortical layer. The deformation of a non-adherent ring under both extracellular and intracellular fluid stresses was solved by a fluid–solid coupled calculation. The deformation of an adherent ring under the adhesion force was calculated by coupling with adhesion bond kinetics (Figs. 2c and d).

The extracellular and intracellular flow fields were calculated using a finite element analysis package (FIDAP; Fluid Dynamics International). It was assumed that fluid surrounding the cell membrane and fluid enclosed by the cell membrane were homogeneous, incompressible and Newtonian (with a different viscosity). Finite element methods were used to solve the two-dimensional steady-state Navier–Stokes equations. The entrance flow was assumed to be a fully developed 2-D Poiseuille flow. At the surface of the lower and upper

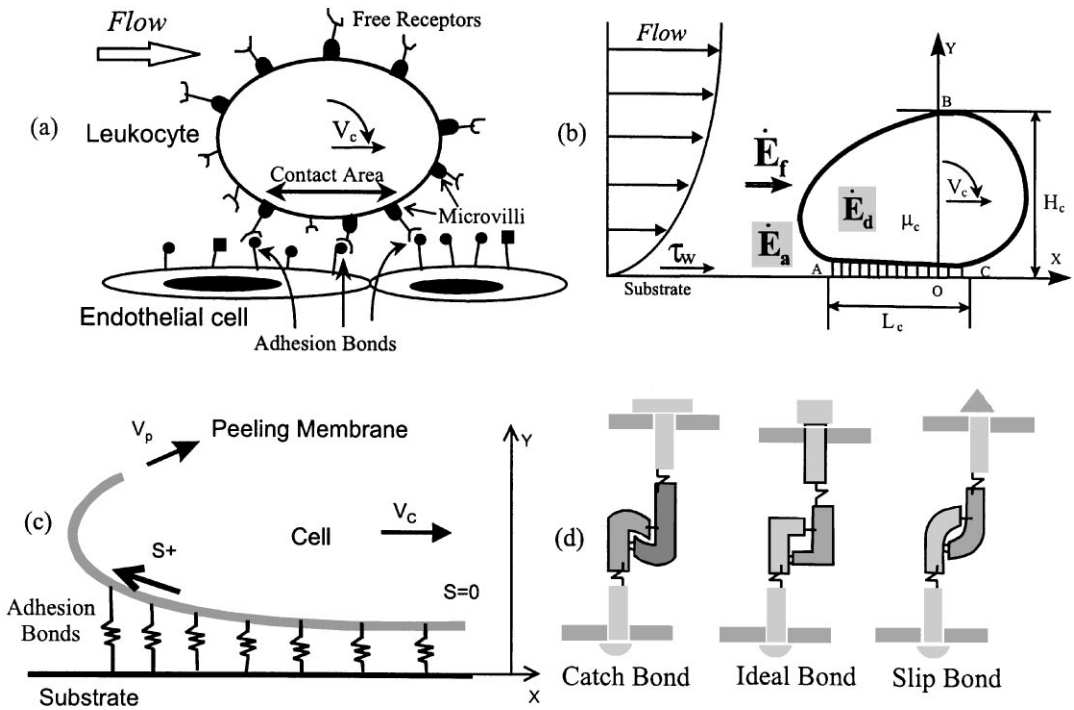

Fig. 2. Model illustrations for a rolling WBC in a shear flow: (a) Factors involved in a rolling WBC interaction with EC, (b) A 2-D cell model in terms of shear stress, cell-surface adhesion and cell deformation. τ_w is the inlet wall shear stress; L_c and H_c are cell contact length and height, respectively; v_c is the cell rolling velocity (i.e. cell center velocity); μ_c is the cytoplasmic viscosity; $\dot{E}_f$, $\dot{E}_d$, and $\dot{E}_a$ are the rates of energy for fluid, viscous cytoplasm, and adhesion bonds, respectively. (c) Illustrations of an adherent membrane and its associated adhesion bonds. v_p is the membrane peeling velocity (relative to the substrate). Microvilli are neglected by assuming all bonds to be spatially distributed along a smooth membrane as a function of s, modeled by elastic springs with constant k (s is the curvilinear coordinate). (d) Schematics of three types of adhesion bonds: (I) Catch bond ($k < k_{ts}$); (II) Ideal bond ($k = k_{ts}$); and (III) Slip bond ($k > k_{ts}$), in which k_{ts} represents the transition state bond elastic constant.

boundaries of the flow channel and of the rolling cell, no slip and no penetration conditions were assumed. The intracellular flow field was solved similarly, with no slip and no penetration boundary conditions for the inner surface of cell membrane. The rate of energy provided by the flow ($\dot{E}_f$) to the rolling cell was

$$\dot{E}_f = \int_{S_f} \sigma_{ij} v_j v_i \, dS = w_c \cdot \int_{C_f} \sigma_{ij} v_j v_i \, ds, \tag{1}$$

where S_f is the surface area exposed to the flow field; C_f is the corresponding 2-D circumference, σ_{ij} is the fluid stress, v_j is the normal unit vector of the surface, and v_i is the velocity on the surface. On the assumption of cell volume conservation, an effective cell width of $w_c = 4R_c/3$ was derived (R_c was the radius of an undeformed cell, which was 3 μm for an average HL-60 cell.).

The rate of energy dissipation of the viscous cytoplasm ($\dot{E}_d$) becomes

$$\dot{E}_d = \int_V \sigma_{ij} \varepsilon_{ij} \, dV = w_c \cdot \int_S \sigma_{ij} \varepsilon_{ij} \, dS, \tag{2}$$

where V is the cell volume, S is the cell cross-sectional area in a 2-D model, and ε_{ij} is the strain rate.

Adhesion kinetic equations were coupled with membrane equations. The cell–substrate contact area was characterized by cell–substrate contact length L_c in the 2-D model. As shown in Fig. 2c, assigning $s = 0$ as the starting point where the adhesion bonds were unstretched, curvilinear coordinate is increased towards the detaching edge. For a rolling cell with no sliding, the rolling velocity v_c (i.e., the cell center velocity) was essentially the membrane detaching velocity v_p (Fig. 2c). The adhesion bond force was assumed to be $f_b = N_b k(y - \lambda)$, where N_b is the bond density, k is the bond elastic constant, λ and y are the lengths of an unstretched bond and a stretched bond, respectively. Dembo et al. (1988) proposed:

$$0 = v_c \frac{\partial N_b}{\partial s} + k_f (N_l - N_b)(N_r - N_b) - k_r N_b, \tag{3}$$

$$k_f = k_{feq} \exp\left(\frac{-k_{ts}(y - \lambda)^2}{2B_z} \right), \tag{4}$$

$$k_r = k_{req} \exp\left(\frac{(k - k_{ts})(y - \lambda)^2}{2B_z} \right), \tag{5}$$

where N_l is the ligand density on the substrate; N_r is cell surface receptor density; k_{feq} and k_{req} are forward and

reverse reaction rate constants for unstretched bonds; B_z is thermal energy, and k_{ts} is the bond elastic constant in transient state. Depending on the values of k_{ts} and k, adhesion bonds could be classified to three types, the so-called catch bonds ($k < k_{ts}$), ideal bonds ($k = k_{ts}$), or slip bonds ($k > k_{ts}$) as defined in Fig. 2d (Dembo et al., 1988). The energy loss in overcoming adhesion ($\dot{E}_a$) was proportional to adhesion bond force and cell rolling velocity

$$\dot{E}_a = w_a \cdot \int_0^{L_c} f_b v_c \frac{\partial y}{\partial s}\, ds, \tag{6}$$

where w_a is the effective width of the contact area ($w_a = \pi L_c/4$, assuming a circular contact area).

Cell rolling velocity, v_c, was calculated based on an energy balance. The rate of energy provided by the surrounding fluid to the rolling cell ($\dot{E}_f$) was assumed to be dissipated predominantly into two parts: $\dot{E}_a$, energy dissipation due to adhesion bond separation, and $\dot{E}_d$, energy loss due to cytoplasm viscous dissipation (Schmid-Schonbein et al., 1987). Other energy gains and losses from biochemical sources during bond association and dissociation were neglected:

$$\begin{aligned}\dot{E}_f(H_c, L_c, \tau_w\,; v_c) &= \dot{E}_a(L_c, N_l, N_r, k, k_{ts}, k_{feq}, k_{req}, \ldots\,; v_c) \\ &\quad + \dot{E}_d(H_c, L_c, \mu_c\,; v_c),\end{aligned} \tag{7}$$

where H_c and L_c are the cell height and cell–surface contact length, respectively. τ_w is the flow wall shear stress along the cell surface and μ_c is the intracellular viscosity.

4. Results

Images of rolling HL-60 cells were recorded, including changes cell height H_c and cell–substrate contact length L_c. H_c and L_c of each rolling cell were measured in three sequential frames and averaged using a video frame grabber (Data Translation, Marlboro, MA). Fig. 1b shows typical video images of a rolling cell under different shear stresses with a substrate P-selectin density of 3.75×10^{10} sites/cm^2. Rolling cell morphologies changed from almost a sphere at a low shear stress to a tear drop-like shape at a high shear stress with an increase in L_c and decrease in H_c (Fig. 3a). However, there were no significant changes in H_c and L_c when P-selectin density N_l changed from 3.75 to 5.3×10^{10} sites/cm^2. HL-60 cell rolling velocities were also measured as a function of shear flow, in terms of cell deformability and P-selectin density (Fig. 3b). With a given ligand density, v_c increased as shear stress increased and seemed to approach a plateau at higher shear stresses. Less change in v_c was seen with a variation of ligand density under low shear stresses (~ 2 dyn/cm^2), but v_c changed more apparently under high shear stresses (~ 20 dyn/cm^2). As ligand density increased, v_c decreased. P-selectin with 3.75 and 5.3 ($\times 10^{10}$ sites/cm^2) were the highest densities that we tested in supporting cell rolling (for $v_c > 0$). In contrast under a high shear stress (20 dyn/cm^2), a value of 0.79 ($\times 10^{10}$ sites/cm^2) was found close to the lowest ligand density to support continuous cell rolling. CB-treated HL-60 cells deformed much more easily than the untreated cells, which resulted in a slower v_c than that of untreated cells. Theoretical predictions on cell deformation and rolling velocity were compared with the experimental measurements (Fig. 3a and b). Values for cytoplasmic viscosity and the adhesion bond reaction rate constants were estimated to derive the fluid drag force and energy dissipation involved in cell rolling under various parametric changes. Some other model

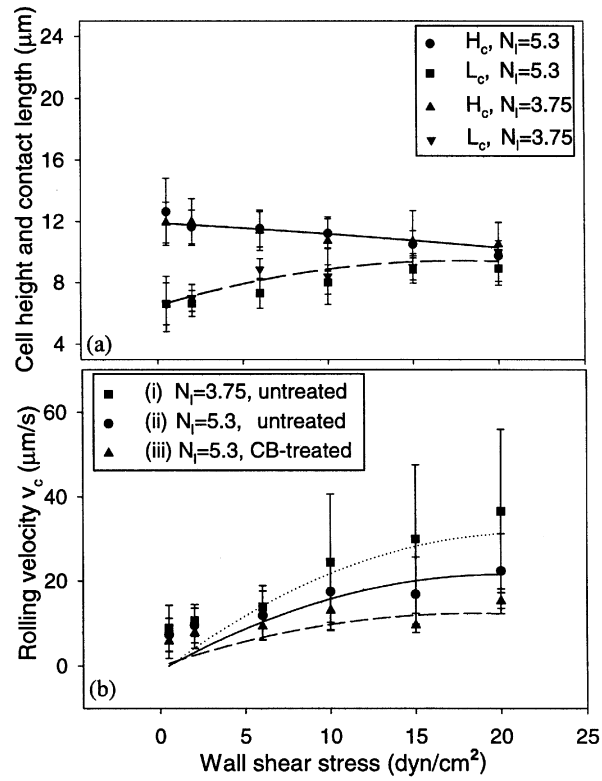

Fig. 3. HL-60 cells roll on a substrate with P-selectin density (N_l; $\times 10^{10}$ sites/cm^2). Data (by symbols) are presented as mean $\pm$ SD averaged from more than 10 cells. Theoretical calculations (by curves) are compared with experiments: (a) Cell height and cell–substrate contact length as a function of shear stresses, influenced by P-selectin density, (b) Cell rolling velocity affected by cell deformability (untreated cells and CB-treated cells) and ligand density under various shear stresses τ_w. The p-value < 0.05 between (i) and (ii) except for very low τ_w (0.5–2.0 dyn/cm^2); and p-value < 0.05 between (ii) and (iii) except for either very low or very high τ_w (0.5 or 15.0–20.0 dyn/cm^2). Cytoplasmic viscosity μ_c was estimated at 40 (CB-treated cells) to 50 (untreated cells) poise to match the measurements on L_c, H_c, and v_c at all shear stress levels tested.

parameters were applied based on previous studies as listed in Table 1.

Shown in Fig. 4a are stress distributions on the surface of a rolling cell. The geometry corners and velocity discontinuity at both detaching edge and attaching edge of the cell caused small fluctuations of the normal stress. The maximum shear stress on the surface of the rolling cell was found to be about 2.8 times the inlet wall shear stress, depending strongly on cell deformation and cell-surface contact. Effects from channel height on the stress distribution was not found to be significant if a channel height was greater than 50 μm (Lei et al., 1999). Drag forces from a sphere parallel to a wall (no contact) are shown in Fig. 4b from both a numerical calculation (2-D) and Goldman's 3-D formula (Goldman et al., 1967). It was found that a rigid sphere separated from the wall by a distance δ (e.g. $\delta = 765$ nm) experienced a greater drag force than that of a sphere or a deformable cell adherent to the wall. A typical distance between leukocyte and endothelium is between 270–765 nm. Only a 7% change in drag force was found when δ increased from 270 to 765 nm.

A rolling cell is driven by fluid forces and hindered by adhesion forces. L_c and v_c are two very important parameters for adhesion energy dissipation ($\dot{E}_a$). As shown in Fig. 5a, $\dot{E}_a$ increased with an increase in L_c or v_p (for a non-slip rolling cell, $v_p = v_c$; Fig. 2c). When v_c became larger, differences in L_c made greater influence on $\dot{E}_a$. Another important factor is the adhesion bond strength. When k_{ts} became smaller than k, indicating slip bonds (Fig. 2d), less $\dot{E}_a$ was needed to detach an adherent cell membrane from its substrate (Fig. 5b). As ligand N_l (P-selectin) density increased, $\dot{E}_a$ would increase initially followed by a plateau at a density around $9–10 \times 10^{10}$ sites/cm^2, in which $\dot{E}_a$ became more invariable to further changes in ligand densities (Fig. 5c). The influence of cell receptor density N_r and kinetic rate constant k_{feq}, k_{req} on $\dot{E}_a$ was also characterized by Fig. 5c, in which both N_r and k_{feq} had more apparent influence, compared with k_{req}, on $\dot{E}_a$.

Fig. 6 shows the fluid energy input $\dot{E}_f$ and percentages of adhesion energy dissipation $\dot{E}_a/\dot{E}_f$ (cytoplasm viscous dissipation $\dot{E}_d/\dot{E}_f = 1 - \dot{E}_a/\dot{E}_f$). In general, $\dot{E}_f$ was found to increase with an increase in shear stress and v_c (Fig. 6a), whereas $\dot{E}_a$ consumed more than 80% of the total fluid energy input (Fig. 6b). With a smaller N_l, cells rolled

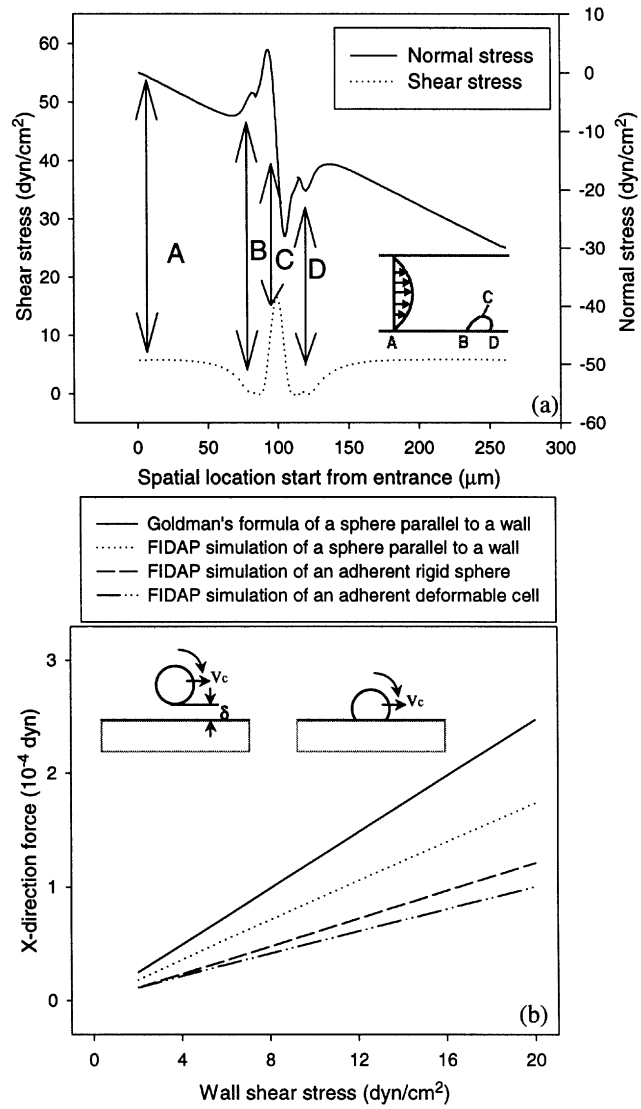

Fig. 4. (a) Stress distributions on the surface of a rolling cell calculated by an inlet wall shear stress 6 dyn/cm^2 and a flow channel height 100 μm. In the 2-D case shown, cell height $H_c = 10.9$ μm; contact length $L_c = 7.37$ μm; contact width $w_c = 4$ μm; and cell rolling velocity $v_c = 20$ μm/s. An insert shows spatial locations represented by A, B, C, and D, (b) Drag force acting, respectively, on a rigid sphere (3-D; $R_c = 3$ μm) parallel to a wall; an adherent rigid sphere (2-D; $R_c = 3$ μm; $w_c = 4$ μm; $H_c = 11.5$ μm; $L_c = 6.15$ μm); and a rolling deformable cell (2-D; $w_c = 4$ μm; $H_c = 11.66–10.17$ μm; $L_c = 6.33–7.35$ μm). Calculations were made using a flow channel height of 100 μm; a gap $\delta = 0.765$ μm; and $v_c = 20$ μm/s. For 2-D cases, an effective cell width $w_c = 4R_c/3$ was used.

Table 1
Model parameters cited: Definitions and values

Symbol	Definition	Value	Reference
N_r	Cell surface receptor density (sites/cm^2)	2.0×10^{10}	Lawrence and Springer (1991)
k_{freq}	Forward reaction rate constant (cm^2/s)	1.0×10^{-9}	Bell (1978)
k_{req}	Reverse reaction rate constant (1/s)	10.0	Bell (1978)
k	Static bond elastic constant (dyn/cm)	0.5	Dembo et al. (1988)
k_{ts}	Transient bond elastic constant (dyn/cm)	0.48	Dembo et al. (1988)
λ	Unstressed bond length (nm)	10.0	Springer (1994)
B_z	Thermal energy (erg)	4.0×10^{-14}	Dembo et al. (1988)

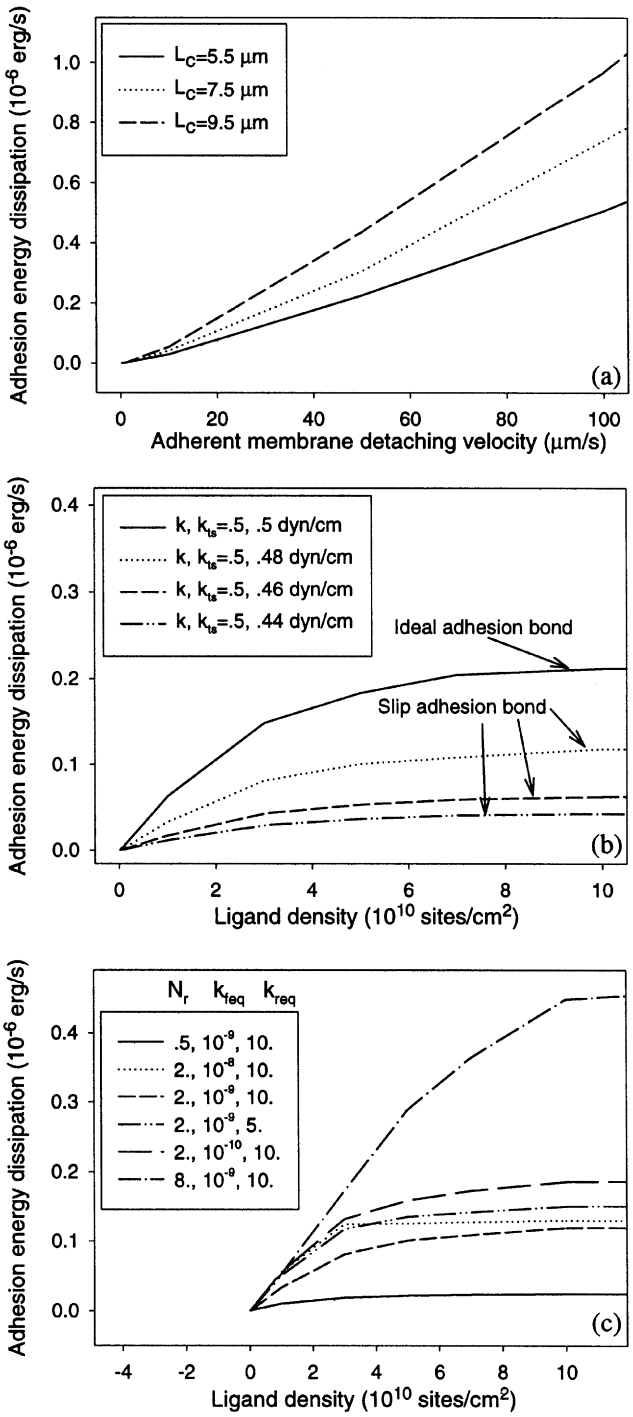

Fig. 5. Adhesion energy dissipation influenced by: (a) membrane detaching velocity (v_p) and cell–substrate contact length, (b) ligand density and receptor–ligand bond elastic constant k and k_{ts} ($k, k_{ts} = 0.5, 0.48$ were used in the current model), (c) receptor density (N_r; $\times 10^{10}$ sites/cm^2), adhesion bond forward reaction rate constant (k_{feq}; cm^2/s), reverse reaction rate constant (k_{req}; 1/s), and ligand density.

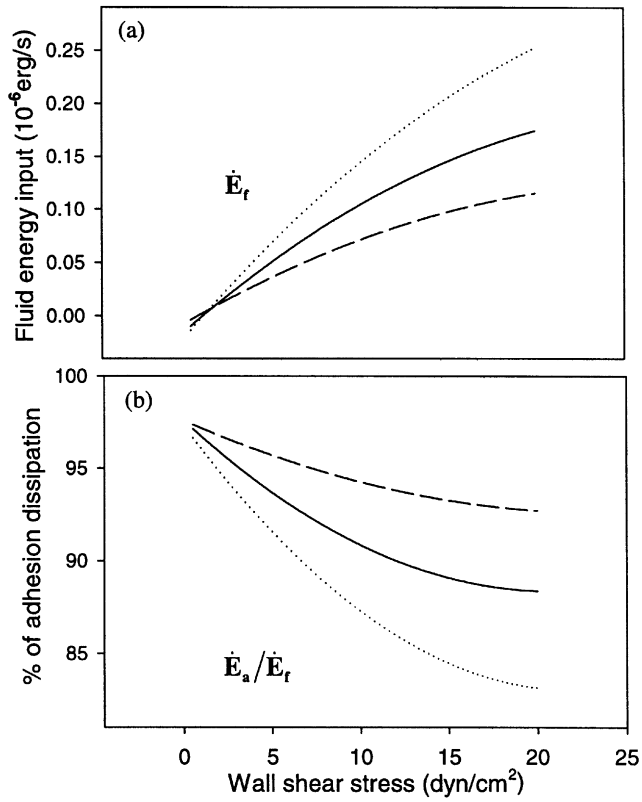

Fig. 6. Ligand density and cell deformability effects on: (a) rate of fluid energy input, (b) percentage of adhesion energy dissipation in fluid energy input, (c) (dotted lines) untreated cells with $N_l = 3.75 \times 10^{10}$ sites/cm^2. (solid lines) untreated cells with ligand density $N_l = 5.3 \times 10^{10}$ sites/cm^2. (dashed lines) CB-treated cells with $N_l = 5.3 \times 10^{10}$ sites/cm^2.

faster resulting in a higher $\dot{E}_f$. More deformable cells (CB-treated) rolled slower, which minimized $\dot{E}_f$. It was found that $\dot{E}_d/\dot{E}_f$ became larger under higher shear stresses, but $\dot{E}_a/\dot{E}_f$ decreased (even though $\dot{E}_a$ increased) as shear stresses increased, suggesting strong influence of cytoplasmic viscous dissipation on cell rolling adhesion under high shear stresses.

Cell deformation and cytoplasmic viscosity μ_c directly affect viscous dissipation, hence, the cell rolling velocity. For example, as μ_c increased from very small values (1–50 poise), v_c decreased rapidly, particularly under high shear stresses (Fig. 7a). However, when μ_c was above 1000 poise, v_c decreased much less with a further increase in μ_c. Fig. 7b shows how adhesion parameters affect cell rolling. For example, v_c was found to be very small (< 1 μm/s) for an ideal bond ($k = k_{ts}$) and less sensitive to changes in wall shear stress. As the adhesion bonds became more slippery ($k_{ts} < k$), cells rolled faster (> 100 μm/s). However, v_c still reached a plateau under higher shear stresses, indicating that a significant increase in cell deformation attenuated a further increase in cell rolling velocity. Fig. 7c shows a dependence of v_c on ligand density with different cell receptor density, forward and reverse rate constants. At a very low N_l (e.g., 10^8 sites/cm^2), v_c was about 200 μm/s that was apparently independent from any changes in N_r, k_{feq} or k_{req}. As

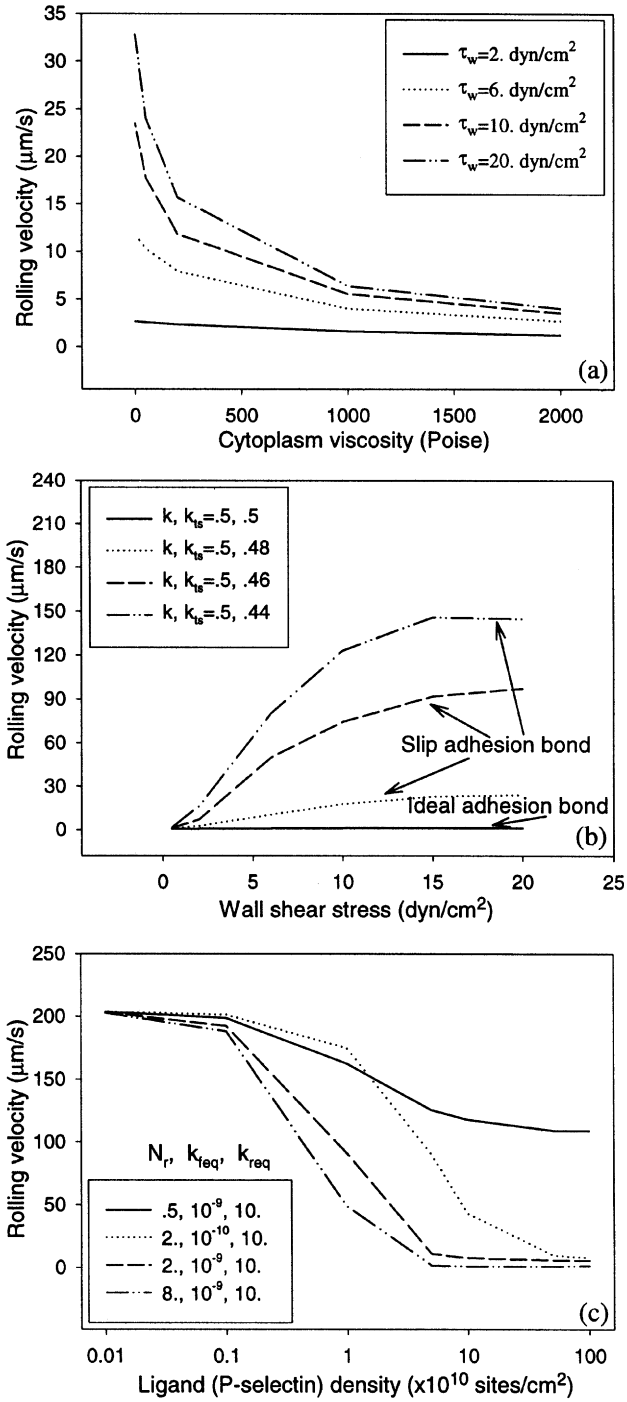

Fig. 7. (a) Effect of cytoplasmic viscosity μ_c on cell rolling velocity under different inlet wall shear stresses. Calculations were made using $N_l = 5.3 \times 10^{10}$ sites/cm^2; $k, k_{ts} = 0.5, 0.48$ dyn/cm, respectively; $N_r = 2 \times 10^{10}$ sites/cm^2; $k_{feq} = 1 \times 10^{-9}$ cm^2/s; and $k_{req} = 10$ 1/s, (b) Influence of adhesion bond constant k and k_{ts} on cell rolling velocity with $\mu_c = 50$ poise. Other parameters are the same as used in (a), (c) Cell rolling velocity as functions of N_r, k_{feq} and k_{req}, with wall shear stress $\tau_w = 6$ dyn/cm^2 and $\mu_c = 50$ poise.

N_l went above 10^9 sites/cm^2, it was found that a 4-fold increase in N_r only downshifted v_c slightly, while a 4-fold decrease in N_r increased v_c by more than 100 μm/s (when $N_l \rightarrow 10^{12}$ sites/cm^2).

5. Discussion

This study presents an in vitro experimental system that allows studies of the relative importance of shear flow, cell-surface adhesion, and cell deformability in cell rolling mechanics. Cell deformation reduces the fluid energy to a cell because a flattened cell causes fewer disturbances to the flow and, hence, smaller shear stresses on the cell surface. Meanwhile, larger cell deformation would result in a larger cell-surface contact area, which leads to more adhesion energy needed to disrupt adhesion bonds and more cytoplasm viscous dissipation required to move the intracellular flow. Such an influence of cell deformation on energy distributions was shown to have a nonlinear effect on cell rolling velocity under various wall shear stresses.

Cytochalasin B is a fungal agent that induces profound changes in cell morphology by inhibition of actin polymerization, and has been found to reduce prestressed tension in the WBC cortical layer and intracellular viscosity (Dong et al., 1999). The WBC cytoplasm is inhomogeneous at all levels of organization and the mechanical properties of the cytoplasm depend on both the magnitude and the rate of applied forces. A more reasonable model of the WBC cytoplasm would be a complex non-Newtonian fluid comprised of an aqueous fluid-phase filling the space within an entangled mesh of filamentous cytoskeletal proteins and other macromolecular structures. If the cytoplasm would be treated as a homogeneous material, the consequence of "apparent" viscosity μ_c may vary greatly, depending significantly on the method of evaluation (Dong et al., 1988; Evans and Yeung, 1989; Lipowsky et al., 1991). Therefore, the values of energy dissipation $\dot{E}_a$ and $\dot{E}_d$ depend on the choice of the cytoplasmic model. In light of the evidence that the cell cytoplasm may behave like a viscoelastic Maxwell fluid, a limiting case for large rolling velocities would lead to a much smaller $\dot{E}_d$. A dependency of cell rolling velocity on the apparent nature of μ_c has been characterized based on the in vitro experiments and model calculations.

An elastic constant at the transit state, k_{ts}, was used to characterize how the rate of bond breakage increases or decreases with extension of the adhesion bond. The magnitude of the difference between k and k_{ts} is important for the micromechanics of an adhesion bond (Fig. 2d). A parameter, $f_k = (k - k_{ts})/k$, is sometimes defined as a "reactive compliance" of an adhesion bond. This quantity relates the strain of a bond to its rate of breakage and indicates a fraction of the energy of bond strain that is actually devoted to breaking tethers. From the present analysis, it was found that with a larger f_k, cell rolling velocity would increase; while if $f_k = 0$, cell rolling velocity would be the slowest. The reaction rate constant k_{feq} and k_{req} were compared with a affinity parameter K_d measured from radioimmunoassay. It has been found

that ^{125}I-labeled soluble forms of P-selectin bind to PSGL-1 on HL-60 cells with an apparent value K_d of 70 nM (Ushiyama et al., 1993). The equilibrium constant for reactants in solution (K_s) is the inverse of K_d. Therefore, $K_s = 1/K_d = 1\ \mathrm{l}/(70 \times 10^{-9}\ \mathrm{mol}) = (1 \times 10^3 \times 10^9\ \mathrm{cm}^3)/(70 \times 6.023 \times 10^{23}) = 2.4 \times 10^{-14}\ \mathrm{cm}^3$. The equilibrium constant for reactants on membranes (K_m) is related to K_s by $K_m = K_s/r_{12}$, where r_{12} is roughly the thickness of a layer parallel to the membrane within which the receptors are located. For PSGL-1 receptors, $r_{12} = 10\ \mathrm{nm} = 10^{-6}\ \mathrm{cm}$, hence $K_m = 2.4 \times 10^{-8}\ \mathrm{cm}^2$ (Bongrand, 1988). The value $k_{eq} = k_{feq}/k_{req}$ we used in this study was $1 \times 10^{-8}\ \mathrm{cm}^2$, which was very close to $K_m = 2.4 \times 10^{-8}\ \mathrm{cm}^2$. The parametric dependence of cell rolling on k_{feq} and k_{req} is presented.

The force to rupture an adhesive bond or extract a receptor from the lipid layer during a cell detaching from the substrate has been estimated to be about 1 μdyn. As for the adhesion energy dissipation per unit area or fracture stress (defined as $\mathrm{d}E_a/\mathrm{d}A_c$), a fracture stress of 0.1 dyn/cm (e.g., under $\dot{E}_a = 10^{-7}$ erg/s, $L_c = 5\ \mu\mathrm{m}$, and $v_c = 20\ \mu\mathrm{m/s}$) was calculated, which agreed with 0.12 erg/cm^2 (= dyn/cm) found by Evans (1985). The adhesion kinetic equations we used in this study assumed that all receptors on the cell surface are immobile and unable to redistribute over the cell surface. Such an assumption is valid for the current analysis based on the Peclet number, $P_e = v_c L/D$, which measures the relative importance of receptor convection and diffusion during cell rolling. For example, with a contact length L of 5 μm and receptor diffusivity D of $10^{-10}\ \mathrm{cm}^2/\mathrm{s}$, $P_e > 50$ was found when rolling velocity $v_c > 0.1\ \mu\mathrm{m/s}$. Therefore, the rolling process is sufficiently fast compared with the receptor mobility on the cell surface. We also applied a set of reaction-limited kinetic equations assuming both forward and reverse reaction rate constants to be independent of ligand density. If the ligand density is very low or the diffusivity of a receptor on the cell surface is high, a diffusion-limited kinetics equation would be more appropriate.

For any cell population, cell properties such as size, deformability, adhesion molecule expression, etc., vary greatly from one cell to another. In the current study, subgroups of HL-60 cells and cells in different growth stages are not distinguished. This certainly will bring many random factors to the experimental data. However, a previous study showed that during HL-60 cell maturation, mechanical properties only changed by a very small range (Tsai et al., 1996). Thus far, no studies have been done for the adhesion molecule expression during cell differentiation. Therefore, with averaged data for cell rolling and deformation, an average level of adhesion molecule expression on cell surface has been assumed. The rolling motion of WBCs fluctuates randomly, and may be due to the heterogeneous effects of adhesion molecule distribution on the cell surface. Stochastic models (Hammer and Apte, 1992; Zhao et al., 1995) showed that experimentally determined rolling velocities depended on the time Δt used in calculating velocities, assuming cell rolling to be a random process. However, with an average rolling cell in mind, we are content at this stage with a deterministic mechanical approach to study the influence of shear flow-induced cell deformation on WBC rolling adhesion. Nevertheless, to illuminate the intriguing details of adhesion receptor–ligand interaction in this process, further studies from both approaches and better yet, combining both approaches in one, are really needed. Some other limitations come from cell surface structure. For example, microvilli with typical length 0.3 μm and spacing 2–3 μm on cell membrane (Bruchl et al., 1996) have been neglected in the present model in detailing a coupled problem between shear flow, cell deformation and adhesion kinetics. Some recent efforts have been made to characterize how much the cell surface roughness would influence a rolling cell, in which rigid spheres covered with microvilli were proposed (Feng et al., 1998; Zhao et al., 1998).

In summary, an in vitro experimental system and a theoretical framework that examines the interaction of shear flow-induced cell deformation and specific adhesion during cell rolling have been presented. The theoretical model incorporates both mechanical aspects of detailed cell deformation and biochemical aspects of adhesion kinetics, and is able to predict cell deformation and rolling velocity quantitatively. From the results predicted by this model, it has been found that shear flow-induced leukocyte deformation could alter the balance between fluid driving force and the adhesion bond force in determining leukocyte rolling adhesion. Due to the many parameters involved in the WBC rolling adhesion process and the difficulties of directly measuring these parameters, better experiment designs with the ability to measure cell deformability and adhesion kinetics are in great need.

Acknowledgements

The authors acknowledge Dr. Michael Lawrence at University of Virginia for providing P-selectin proteins. This study was supported in part by the Whitaker Foundation research grant and the NSF Career Award BES-9302079.

References

Bell, G.I., 1978. Models for the specific adhesion of cells to cells. Science 200, 618–627.

Bongrand, P. (Ed.) 1988. Physical basis of cell–cell adhesion, CRC Press, Inc. Boca Raton, FL.

Bruehl, R.E., Springer, T.A., Bainton, D.F., 1996. Quantitation of L-selectin distribution on human leukocyte microvilli by immunogold labeling and electron microscopy. Journal of Histochemistry Cytochemistry 44, 835–844.

Cao, J., Donell, B., Deaver, D.R., Lawrence, M.B., Dong, C., 1998. In Vitro side-view imaging technique and analysis of human T-leukemic cell adhesion to ICAM-1 in shear flow. Microvascular Research 55, 124–137.

Cao, J., Usami, S., Dong, C., 1997. Development of a side-view chamber for studying cell-surface adhesion under flow conditions. Annals of Biomedical Engineering 25, 573–580.

Dembo, M., Torney, D.C., Saxman, K., Hammer, D., 1988. The Reaction-limited kinetics of membrane-to-surface adhesion and detachment. Proceedings of Royal Society of London B 234, 55–83.

Dong, C., Cao, J., Struble, E.J., Lipowsky, H.H., 1999. Mechanics of leukocyte deformation and adhesion to endothelium in shear flow. Annals of Biomedical Engineering 27, 298–312.

Dong, C., Skalak, R., Sung, K.-L.P., Schmid-Schoenbein, G.W., Chien, S., 1988. Passive deformation analysis of human leukocytes. Journal of Biomedical Engineering 110, 27–36.

Evans, E.A., 1985. Detailed mechanics of membrane–membrane adhesion and separation I. Continuum of molecular cross-bridges. Biophysics Journal 48, 175–183.

Evans, E., Yeung, A., 1989. Apparent viscosity and cortical tension of blood granulocytes determined by micropipet aspiration. Biophysics Journal 56, 151–160.

Feng, J., Ganatos, P., Weibaum, S., 1998. Motion of a sphere near planar confining boundaries in a Brinkman medium. Journal of Fluid Mechanics 375, 265–296.

Goldman, A.J., Cox, R.G., Brenner, H., 1967. Slow viscous motion of a sphere parallel to a plane wall—I. Motion through a quiescent fluid. Chemical Engineering Science 22, 637–651.

Hammer, D.A., Apte, S.M., 1992. Simulation of cell rolling and adhesion on surfaces in shear flow: general results and analysis of selectin-mediated neutrophil adhesion Biophysics Journal 63, 35–57.

Lauffenberger, D.A., Linderman, J.J., 1993. Receptors: Models for binding, trafficking, and signaling. Oxford University Press, New York.

Lawrence, M.B., Kansas, G.S., Kunkel, E.J., Ley, K., 1997. Threshold levels of fluid shear promote leukocyte adhesion through selectins (CD62LP, E). Journal of Cell Biology 136, 717–727.

Lawrence, M.B., Springer, T.A., 1991. Leukocytes roll on a selectin at physiologic flow rates: distinction from and prerequisite for adhesion through integrins. Cell 65, 859–873.

Lei, X.X., Lawrence, M.B., Dong, C., 1999. Influence of cell deformation on leukocyte rolling adhesion in shear flow. ASME — Journal of Biomechanical Engineering, 121, in press.

Lipowsky, H.H., Riedel, D., Shi, G.S., 1991. In Vivo mechanical properties of leukocytes during adhesion to venular endothelium. Biorheology 28, 53–64.

Schmid-Schoenbein, G.W., Skalak, R., Simon, S.I., Engler, R.L., 1987. The interaction between leukocytes and endothelium in vivo. Ann. New York Academy of Science 516, 348–361.

Springer, T.A., 1994. Traffic signals for lymphocyte recirculation and leukocyte emigration: the multistep paradigm. Cell 76, 301–314.

Tsai, M.A., Wauch, R.E., Keng, P.C., 1996. Changes in HL-60 cell deformability during differentiation introduced by DMSO. Biorheology 33, 1–15.

Ushiyama, S., Laue, T.M., Moore, K.L., Erickson, H.P., McEver, R.P., 1993. Structural and functional characterization of monnmeric soluble P-selectin and comparision with membrane P-selectin. Journal of Biological Chemistry 268, 15229–15237.

Zhao, Y., Chien, S., Weinbaum, S., 1998. Hydrodynamics of leukocyte tether interaction and a model for the L-selectin shear threshold. Annals of Biomedical Engineering 26, S74 (Abstract).

Zhao, Y., Chien, S., Skalak, R., 1995. A Stochastic model of leukocyte rolling. Biophysics Journal 69, 1–12.